RSC Advances

PAPER

View Article Online
View Journal | View Issue

Cite this: *RSC Adv.*, 2019, **9**, 27386

Photoluminescence and afterglow behavior of Ce^{3+} activated $Li_2Sr_{0.9}Mg_{0.1}SiO_4$ phosphor

Yingjun Xiao, Dongyun Zhang * and Chengkang Chang *

Received 5th July 2019
Accepted 14th August 2019

DOI: 10.1039/c9ra05093k

rsc.li/rsc-advances

A blue emitting phosphor $Li_2Sr_{0.9}Mg_{0.1}SiO_4:Ce^{3+}$, with long persistence, was synthesized *via* a high-temperature solid phase method. According to the X-ray diffraction analysis result, the introduction of Mg^{2+} and Ce^{3+} ions has no influence on the structure of the host material. Typical 5d-$^2F_{5/2}$ and 5d-$^2F_{7/2}$ transitions of Ce^{3+} ions were detected by PL spectra, which corresponded to the CIE chromaticity coordinates of $x = 0.1584$, $y = 0.0338$. An optimal doping concentration of Ce^{3+} was determined as of 0.4 at%. Furthermore, the $Li_2Sr_{0.9}Mg_{0.1}SiO_4:Ce^{3+}$ phosphor showed a typical triple-exponential afterglow behavior when the UV source was switched off. The highest lifetime of the electrons within the material reached a value of 73.9 s. Thermal stimulated luminescence study indicated that the afterglow of $Li_2Sr_{0.9}Mg_{0.1}SiO_4:Ce^{3+}$ was due to the recombination of the electrons with holes released from the traps generated by the doping of Ce^{3+} ions in the $Li_2Sr_{0.9}Mg_{0.1}SiO_4$ host. The afterglow mechanism of $Li_2Sr_{0.9}Mg_{0.1}SiO_4:Ce^{3+}$ is illustrated and discussed in detail on the basis of the experimental results.

1. Introduction

Long-lasting phosphors (LLPs) are a kind of energy storage materials with the decay time extended to seconds, minutes, or even hours after the removal of ultraviolet (UV) and visible light at room temperature.[1–4] These materials have been widely studied by many researchers because of their excellent properties, such as long persistence time, stable crystal structure, high physical and chemical stabilities.[5–8] The most commonly used long lasting phosphors (LLPs) are $CaAl_2O_4:Eu^{2+}$, Nd^{3+} (blue), $SrAl_2O_4:Eu^{2+}$, Dy^{3+} (green) and $Y_2O_2S:Eu^{3+}$, Ti^{4+}, Mg^{2+} (red).[9,10] It is generally agreed that long luminescence lifetimes can be achieved by adjusting the host crystal bandgap and the energy level by introducing rare-earth ions. However, it is difficult to generate an appropriate trap depth in these host materials; hence, the progress in this field is quite slow. Therefore, extensive studies still need to be carried out in order to achieve the best performance of the long-lasting phosphorescent materials.

Recently, a lithium silicate system has been regarded as a suitable host with high chemical stability, and it can produce a suitable crystal environment imposing on the emission centers. Thus, such system has been widely investigated and silicate phosphors with various colors have been well recorded in documents.[11–17] We also reported some LLPs in the silicate system, where Li_2SrSiO_4 and $Li_2Ca_{0.6}Sr_{0.4}SiO_4$ were suggested as excellent hosts for LLPs.[18,19]

It is also recommended that the phosphorescence of Ce^{3+} in most of the hosts is caused by the 5d-$^2F_{5/2}$ and 5d-$^2F_{7/2}$ energy-level transitions.[20–23] However, there has been no detailed report on the long lasting phosphorescence phenomenon of Ce^{3+} in lithium silicate phosphors. To understand the afterglow behavior of the Ce^{3+} doped lithium silicate phosphors, it is important to find a suitable host crystal with a certain bandgap that matches with the energy level of the Ce^{3+} ions. In this study, a series of blue emitting LLPs $Li_2Sr_{0.9}Mg_{0.1}SiO_4:x\%$ Ce^{3+} (x = 0.1, 0.2, 0.3, 0.4, and 0.5), was investigated to carry out the survey. The results demonstrated that it was the Ce^{3+} ions incorporated into the substrate that caused the afterglow. Thermal stimulated luminescence study indicated that the afterglow of $Li_2Sr_{0.9}Mg_{0.1}SiO_4:Ce^{3+}$ was due to the recombination of the electrons with holes released from the traps generated by the doping of Ce^{3+} ions in the $Li_2Sr_{0.9}Mg_{0.1}SiO_4$ host and we discussed the long-lasting phosphorescent phenomenon in detail by means of a completely trapping model.

2. Experimental procedures

2.1 Sample synthesis

The $Li_2Sr_{0.9}Mg_{0.1}SiO_4:Ce^{3+}$ phosphor was prepared by the traditional high-temperature solid phase reaction, using the raw materials, $SrCO_3$, Li_2CO_3, MgO, SiO_2, and CeO_2, each with a purity of 99.99%. The Ce^{3+} doping level ranged from 0.1%, 0.2%, 0.3%, 0.4% to 0.5%. The raw materials were mixed in stoichiometric ratios, ground for 1 h and finally sintered at 850 °C under a weak reductive atmosphere (5% H_2 + 95% N_2). The samples were kept at this temperature for 10 h and then cooled to room temperature while maintaining the flow of the reducing gas till the furnace reached room temperature.

School of Materials Science and Engineering, Shanghai Institute of Technology, 100 Haiquan Road, Shanghai 200235, China. E-mail: dyz@sit.edu.cn; ckchang@sit.edu.cn

2.2 Characterization

X-ray diffraction was performed using a TD-3500 X-ray diffractometer with Cu K_α irradiation to collect the crystal information of the as-prepared phosphors. A Hitachi F7000 fluorescence spectrophotometer was used to detect the excitation and emission spectra of the samples. The afterglow behavior and the trap energy level determinations were measured using an FJ427-A1 thermally stimulated spectrometer.

3. Results and discussion

3.1 Phase identification

The phase and structure of the samples were determined using X-ray powder diffraction. Fig. 1 indicates the composition of $Li_2Sr_{0.9}Mg_{0.1}SiO_4$ phosphors doped with different concentrations of Ce^{3+} (0.1%, 0.3% and 0.5%), which are compared to the standard file from the JCPDS card no. 047-120. It is possible to suggest that the peaks of the samples correspond to single hexagonal phase.[11] Despite the increase in the Ce^{3+} dopant concentration (up to 0.5%), no other product was observed. The possible reason is that the radius of Ce^{3+} ions ($r = 1.196$ Å) being very close to that of Sr^{2+} (1.31 Å), the Ce^{3+} ions are expected to occupy the Sr^{2+} sites in the $Li_2Sr_{0.9}Mg_{0.1}SiO_4$ host lattice. It can be concluded from the results that the doped Ce^{3+} ions as well as Mg^{2+} ions, have been successfully incorporated into the lattice of the silicate compound, and the co-doping of Ce^{3+} and Mg^{2+} ions did not disturb the host crystal lattice.

3.2 Photoluminescence properties

Fig. 2 portrays the photoluminescence behavior of the $Li_2Sr_{0.9}Mg_{0.1}SiO_4$:0.004$Ce^{3+}$ phosphor. A typical photoluminescence excitation and emission spectra of 0.4 at% Ce^{3+} activated $Li_2Sr_{0.9}Mg_{0.1}SiO_4$ phosphor is shown in Fig. 2a. From the PLE spectrum, a broad band is observed in the wavelength region of 250–350 nm, centering at about 277 nm and located at 253 nm, 276 nm and 314 nm respectively, which originates from the 5d → 4f transition of the Ce^{3+} ions.[24,25] As we can see, the emission spectra of the phosphor consist of two bands, peaking at 391 and 416 nm in the wavelength region of 350–550 nm under the excitation of 277 nm. Such emissions are typical for that of Ce^{3+} ascribed to the 5d-$^2F_{5/2}$ and 5d-$^2F_{7/2}$ transitions. Fig. 2b shows the corresponding CIE 1931 chromaticity diagram of the $Li_2Sr_{0.9}Mg_{0.1}SiO_4$:0.004$Ce^{3+}$ phosphor. Point with chromaticity coordination ($x = 0.1584$, $y = 0.0338$) is located in the region of the blue color, indicating that the color of LLL in $Li_2Sr_{0.9}Mg_{0.1}SiO_4$:0.004$Ce^{3+}$ is blue. In our study, the high quantum efficiency of the PL emission yields of up to 60% at 300 K were obtained. The value of the quantum efficiency in this case is higher than the Eu^{2+} ions as activator in the Li_2SrSiO_4 matrix in ref. 26, which means that the Ce^{3+} as an activator in the $Li_2Sr_{0.9}Mg_{0.1}SiO_4$ matrix is superior and valuable.

The effects of doping concentration on the PL properties were further investigated. When being excited by 277 nm, the emission spectra of $Li_2Sr_{0.9}Mg_{0.1}SiO_4$:$Ce^{3+}$ phosphors with different concentrations of Ce^{3+} are depicted in Fig. 3. It can be observed that the emission intensity of $Li_2Sr_{0.9}Mg_{0.1}SiO_4$:$Ce^{3+}$ increases initially with an increase in the Ce^{3+} concentration, and then decreases with a maximum intensity reaching at a doping concentration of 0.4 at%. This phenomenon results from the concentration quenching, which was studied by Chen.[27] These results demonstrate that the optimal doping concentration of Ce^{3+} in $Li_2Sr_{0.9}Mg_{0.1}SiO_4$ experimentally determined to be 0.4 at%.

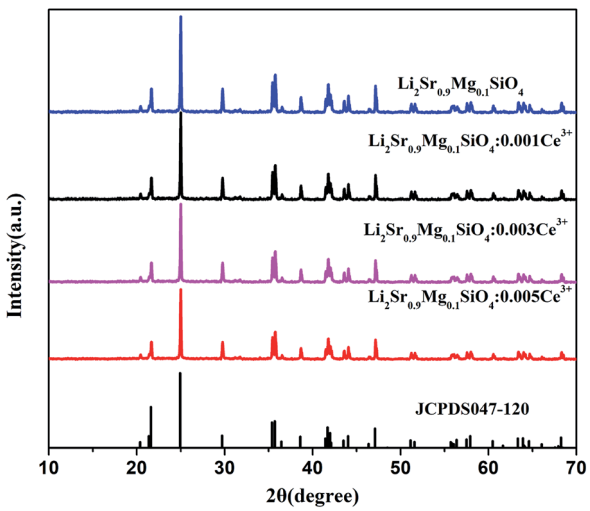

Fig. 1 XRD patterns of $Li_2Sr_{0.9}Mg_{0.1}SiO_4$ and $Li_2Sr_{0.9}Mg_{0.1}SiO_4$:$Ce^{3+}$.

3.3 Long afterglow properties

As mentioned above, the $Li_2Sr_{0.9}Mg_{0.1}SiO_4$:0.004$Ce^{3+}$ phosphors show a blue emission when excited under an ultraviolet source of 277 nm and exhibit long-lasting phosphorescence. The room-temperature decay curves of the long afterglow phosphorescence of $Li_2Sr_{0.9}Mg_{0.1}SiO_4$:0.004$Ce^{3+}$ are depicted in Fig. 4. The decay characteristics of the $Li_2Sr_{0.9}Mg_{0.1}SiO_4$:0.004$Ce^{3+}$ phosphor can be roughly divided into two processes, the rapid-decay process and the slow-decay process. The decay curves of the afterglow of the phosphors can be evaluated by the curve fitting technique. In this study, a triple-exponential equation, which has been used widely, can fit the experimental decay curves very well:[28]

$$I = I_0 + A_1 \exp\left(-\frac{t}{\tau_1}\right) + A_2 \exp\left(-\frac{t}{\tau_2}\right) + A_3 \exp\left(-\frac{t}{\tau_3}\right) \quad (1)$$

where I_0 is the persistent luminescence intensity at time 0; A_1, A_2 and A_3 are the constants; t is the time, and τ_1, τ_2, τ_3 are the decay times for the rapid-decay and slow-decay components. Fig. 4 reveals the results of the fitting curve, with the maximum value (τ_3) reaching 73.9 s. It is known that the bigger the value of the decay time is, the slower the decay rate and the better the afterglow properties are.[29,30] The results imply that the Ce^{3+} ion-doped phosphor possesses a good persistence although the phosphor showed a rapid decay at the initial process.

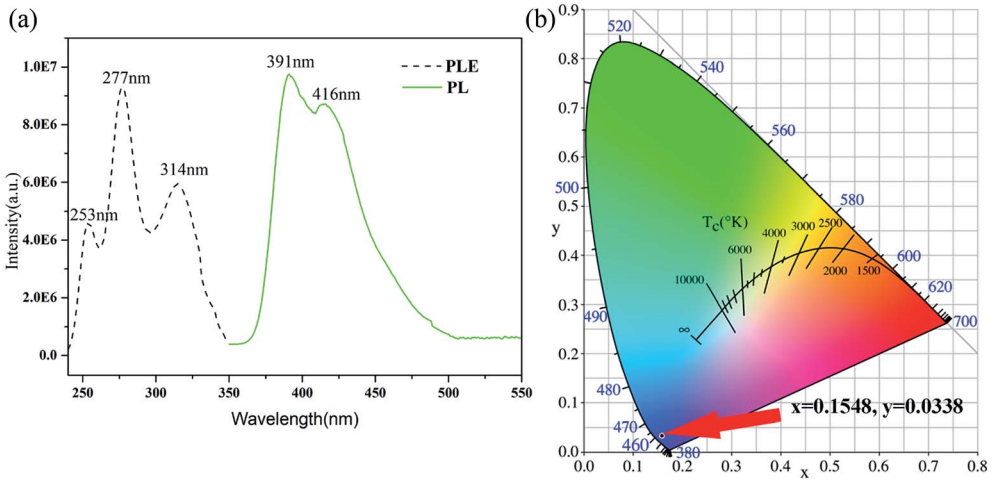

Fig. 2 PLE and PL (λ_{ex} = 277 nm) spectra (a), and CIE 1931 chromaticity coordinates of the $Li_2Sr_{0.9}Mg_{0.1}SiO_4$:0.004$Ce^{3+}$phosphor (b).

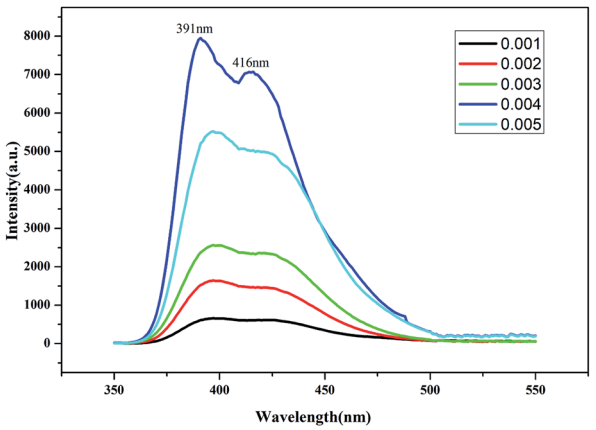

Fig. 3 PL (λ_{ex} = 290 nm) spectra of $Li_2Sr_{0.9}Mg_{0.1}SiO_4$:$Ce^{3+}$ phosphors.

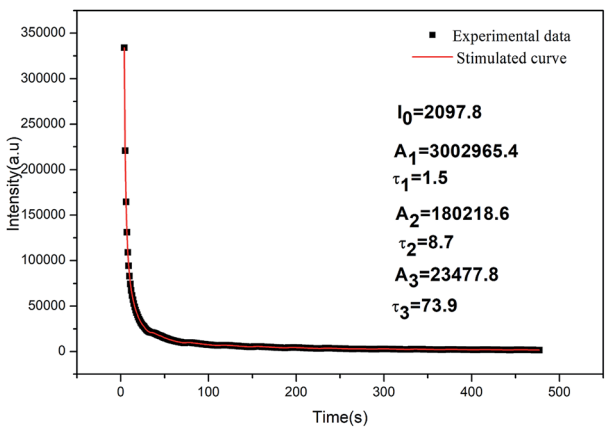

Fig. 4 Afterglow curve of the Li_2SrSiO_4:0.004Ce^{3+} phosphor.

3.4 Thermoluminescence performance

In order to further investigate the nature of the trap in $Li_2Sr_{0.9}Mg_{0.1}SiO_4$:0.004$Ce^{3+}$, thermoluminescence studies were carried out. The thermoluminescence curves indicating the integrated emission intensity is depicted in Fig. 5. As we all know, a proper energy level of the traps is essential for good afterglow properties and the depth of traps and the trap density in the phosphors can be dealt with the equation:[31,32]

$$I(T) = sn_0 \exp\left(-\frac{E_t}{KT}\right)\left[\left(\frac{(l-1)s}{\beta}\right)\right.$$

$$\left.\times \int_{T_0}^{T} \exp\left(-\frac{E_t}{KT}\right)dT + 1\right]^{-l/(l-1)} \quad (2)$$

where $I(T)$ is the TL intensity, s the frequency factor, n_0 is the trap concentration of trap charges $t = 0$, E_t is the trap depth, k is the Boltzmann's constant, l is the kinetics order and b is the heating rate (1 °C s^{-1} in the experiment). In our study, the parameters s, n_0, E_t and l were obtained by a computer fitting technique.[30] The thermoluminescence behavior can be analyzed by curve fitting as referred by Chen, relying on the following exponential equation:[33,34]

$$\int_{T_0}^{T} \exp\left(-\frac{E_t}{KT}\right)dT = T\exp\left(-\frac{E_t}{KT}\right)\sum_{j=1}\left(-\frac{E_t}{KT}\right)^j(-1)^{j-1}j! \quad (3)$$

j is conceded to be 3 in this case and we got another eqn (4):

$$\int_{T_0}^{T} \exp\left(-\frac{E_t}{KT}\right)dT = T\exp\left(-\frac{E_t}{KT}\right)\left(\frac{KT}{E_t} - 2\left(\frac{KT}{E_t}\right)^2\right.$$

$$\left.+ 6\left(\frac{KT}{E_t}\right)^3\right) \quad (4)$$

The calculated trap depth and density of $Li_2Sr_{0.9}Mg_{0.1}SiO_4$:0.004$Ce^{3+}$ phosphors are shown in Fig. 5. The trap level and trap concentrations are two useful indicators to evaluate the long duration phosphorescence of different phosphors. Having an electron trap of suitable energy level is necessary to create the afterglow behavior. The asymptotes can be found practically in all experiments, where the values of I, S and E are between 0.7 and 2.5, between 10^5 s^{-1} and 10^{13} s^{-1}, and between 0.1 and 1.6 eV, respectively. In this case, the corresponding

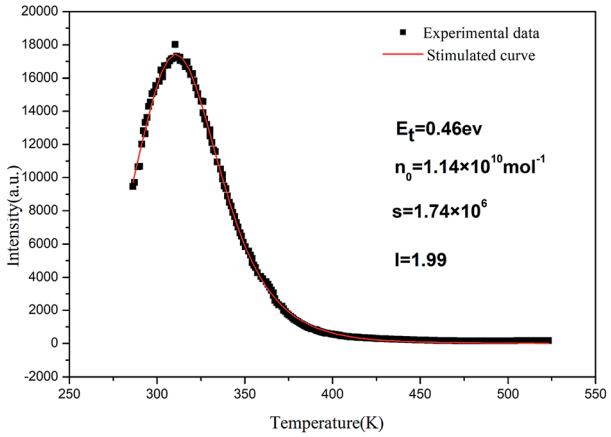

Fig. 5 TSL curve of the $Li_2Sr_{0.9}Mg_{0.1}SiO_4$:0.004$Ce^{3+}$ phosphor.

values were in these ranges. It is well known that the trap created by the lattice defects play a very important role on the afterglow properties of the phosphors. According to Kuang's report, the trap depths should lie between 0.4 and 0.6 eV if the materials are to show excellent persistent phosphorescence performance.[35] The calculated trap concentration was 1.14 × 10^{10} mol^{-1} and the depth of the trap energy level of $Li_2Sr_{0.9}Mg_{0.1}SiO_4$:0.004$Ce^{3+}$ was 0.46 eV, which were very close to the values reported. We observed that the trap depth of 0.46 eV for 0.4 at% Ce^{3+} doped $Li_2Sr_{0.9}Mg_{0.1}SiO_4$ is suitable for excellent afterglow at room temperature.

3.5 Possible mechanism of persistence

Based on the above description and analyses, we are trying to elucidate the phosphorescence mechanism of $Li_2Sr_{0.9}Mg_{0.1}SiO_4$:$Ce^{3+}$. In Ce^{3+}-doped phosphor, it seems reasonable that the Ce^{3+} (r = 1.196 Å) ions are expected to occupy the incorporated Sr^{2+} (r = 1.31 Å) sites of the $Li_2Sr_{0.9}Mg_{0.1}SiO_4$ host due to their close ionic radius. The replacement can be explained by the mechanism: $2Ce^{3+} + 3Sr^{2+} \rightarrow 2Ce_{Sr}^{\bullet} + V_{Sr}''$. In order to maintain the charge balance, it is the only replacement way possible, as three Sr^{2+} ions can be replaced by two Ce^{3+} ions, which induce two positive defects $Ce_{Sr}^{\bullet}$ and one negative defect $V_{Sr}^{\bullet}$ in the host. In our case, on the basis of our PL spectra and TL analysis results, Ce^{3+} not only acts as the luminescent center in the host lattice, but also serves as the trap center.

The detailed mechanism of the long-lasting phosphorescence is yet to be known. The afterglow of Ce^{3+} doped in the $Li_2Sr_{0.9}Mg_{0.1}SiO_4$ phosphor and the cause of such phenomenon was assumed to be due to the thermo-stimulated recombination of the holes at the traps induced by irradiation, which leave the holes or the electrons in a meta-stable excited state at room temperature. Based on the above results, a simple mechanism for the LLP of $Li_2Sr_{0.9}Mg_{0.1}SiO_4$:$Ce^{3+}$ is proposed, which is presented in Fig. 6. Upon UV-irradiation (step 1), the electrons in the valence band are excited to the conduction band, resulting in the formation of free electrons and holes at the same time in the phosphor. Then, the energy associated with the excited electrons is transferred to the 5d level of Ce^{3+}. The subsequent jumping of electron traps to the ground level $^2F_{5/2}$ and $^2F_{7/2}$ states of Ce^{3+} and the recombination of holes give rise to the characteristic emission of Ce^{3+} ions (step 2 and step 5). In this process, a number of free holes and excited electrons can be captured by the $Ce_{Sr}^{\bullet}$ and $V_{Sr}^{\bullet}$ trapping centers (step 3). After the UV irradiation is removed, these electrons trapped by Ce^{3+} will be released from the traps and transferred *via* the host to the luminescence center (step 4), followed by the recombination of free electrons and holes, leading to the characteristic emission of Ce^{3+} ions (step 5). When the decay ratio of the carries released from the electron traps to the 5d state of the Ce^{3+} ions is proper, the blue-emitting LLP of Ce^{3+} can be obtained.

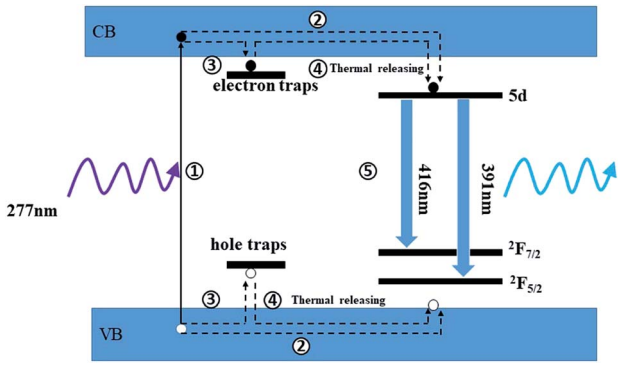

Fig. 6 Schematic graph of phosphorescence mechanism. ○ represent hole; ● represent electron.

4. Conclusions

In summary, a kind of blue-emitting long afterglow phosphor $Li_2Sr_{0.9}Mg_{0.1}SiO_4$:$Ce^{3+}$ was successfully synthesized by the traditional high-temperature solid phase reaction. The doping of Ce^{3+} had no influence on the $Li_2Sr_{0.9}Mg_{0.1}SiO_4$ lattice. Upon UV illumination, typical 5d-$^2F_{5/2}$ and 5d-$^2F_{7/2}$ transitions from Ce^{3+} ions were observed by PL spectra, and the optimal doping concentration for Ce^{3+} of 0.4 at% was determined. After the UV irradiation was removed, an afterglow was observed from the $Li_2Sr_{0.9}Mg_{0.1}SiO_4$:$Ce^{3+}$ phosphor, which was later confirmed in terms of the triple-exponential model with a maximum lifetime value (τ_3) of 73.9 s. The LLP phenomenon of the matrix was supposed to be caused by the thermo-stimulated recombination of holes and free electrons, which were released from the trapped metastable state at room temperature.

Conflicts of interest

There are no conflicts to declare.

References

1 Y. Lin, Z. Tang and Z. Zhang, Preparation of long-afterglow $Sr_4Al_{14}O_{25}$ based luminescent material and its optical properties, *Mater. Lett.*, 2001, **51**, 14–18.
2 Y. Lin, Z. Tang and Z. Zhang, Preparation of a new long afterglow blue-emitting $Sr_2MgSi_2O_7$-based photoluminescent phosphor, *J. Mater. Sci. Lett.*, 2001, **20**, 1505–1506.

3 X. Wang, Z. Zhang and Z. Tang, Characterization and properties of a red and orange Y_2O_2S-based long afterglow phosphor, *Mater. Chem. Phys.*, 2003, **80**, 1–5.

4 I. Ahemen and F. B. Dejene, Spectroscopic Investigation of Ce^{3+}/Eu^{3+} Co-Doped Li2bazro4 Nanocrystalline Phosphors, *J. Alloys Compd.*, 2018, **735**, 2436–2445.

5 Y. Chen, X. Cheng, M. Liu, *et al.*, Comparison study of the luminescent properties of the white-light long afterglow phosphors: $CaxMgSi_2O_{5+x}$: Dy^{3+}(x= 1, 2, 3), *J. Lumin.*, 2009, **129**, 531–535.

6 Y. Jin, Y. Hu, L. Chen, X. Wang, Z. Mu, G. Ju and T. Wang, A novel orange emitting long afterglow phosphor $Ca_3Si_2O_7$: Eu^{2+} and the enhancement by R^{3+} ions (R= Tm, Dy and Er), *Mater. Lett.*, 2014, **126**, 75–77.

7 J. Ding, Q. Wu and Y. Li, Self-Activated Yellow Light Emitting Phosphors of α, β-$Ca_3B_2N_4$ with Long Afterglow Properties, *Inorg. Chem.*, 2016, **55**, 10990–10998.

8 T. Cui, P. Ma, Y. Sheng, *et al.*, Preparation of $CaAl_2O_4$: Eu^{2+}, Nd^{3+} and $SrAl_2O_4$: Eu^{2+}, Dy^{3+} long afterglow luminescent materials using oil shale ash, *Opt. Mater.*, 2017, **67**, 84–90.

9 W. Li, Y. Liu and P. Ai, Synthesis and luminescence properties of red long-lasting phosphor Y_2O_2S:Eu^{3+}, Mg^{2+}, Ti^{4+} nanoparticles, *Mater. Chem. Phys.*, 2010, **119**, 52–56.

10 Y. Mei, H. Xu, J. Zhang, Z. Ci, M. Duan and S. Peng, Design and spectral control of a novel ultraviolet emitting long lasting phosphor for assisting TiO_2photocatalysis: Zn_2SiO_4:Ga^{3+}, Bi^{3+}, *J. Alloys Compd.*, 2015, **622**, 908–912.

11 M. P. Saradhi and U. V. Varadaraju, Photoluminescence studies on Eu^{2+} activated Li_2SrSiO_4 a potential orange-yellow phosphor for solid-state lighting, *Chem. Mater.*, 2006, **18**, 5267–5272.

12 S. M. Levshov, I. V. Berezovskaya and N. P. Efryushina, Synthesis and luminescence properties of Eu^{2+} doped Li_2SrSiO_4, *Inorg. Mater.*, 2011, **47**, 285–289.

13 J. Liu, J. Sun and C. Shi, A new luminescent material: Li_2CaSiO_4:Eu^{2+}, *Mater. Lett.*, 2006, **60**, 2830–2833.

14 S. Cheng, X. Xu, J. Han, J. Qiu and B. Zhang, Design, synthesis and characterization of a novel orange-yellow long-lasting phosphor: Li_2SrSiO_4:Eu^{2+}, Dy^{3+}, *Powder Technol.*, 2015, **276**, 129–133.

15 P. You, Effect of Tb^{3+}doped Concentration on Properties of Li_2SrSiO_4:Tb^{3+} Phosphor, *Adv. Mater. Res.*, 2014, **919**, 2052–2056.

16 E. Erdoğmuş, I. Pekgözlü and E. Korkmaz, Synthesis and Photoluminescence Properties of Li_2SrSiO_4: Pb^{2+}, *J. Appl. Spectrosc.*, 2014, **81**, 336–340.

17 H. He, R. Fu, Y. Cao, *et al.*, $Ce^{3+} \rightarrow Eu^{2+}$ energy transfer mechanism in the Li_2SrSiO_4:Eu^{2+}, Ce^{3+} phosphor, *Opt. Mater.*, 2010, **32**, 632–636.

18 X. Y. Li, D. Y. Zhang, Y. Chen and C. K. Chang, Preparation and characterization of a green emitting $Li_2Ca_{0.4}Sr_{0.6}SiO_4$: Tb^{3+} phosphor with afterglow behavior, *Ceram. Int.*, 2017, **43**, 1677–1681.

19 X. Y. Li, D. Y. Zhang and C. K. Chang, Preparation and characterization of orange -yellow emitting $Li_2Ca_{0.4}Sr_{0.6}SiO_4$: Eu^{2+}, Dy^{3+} phosphor with afterglow behavior, *J. Lumin.*, 2017, **183**, 48–52.

20 W. R. Liu, C. H. Huang, C. P. Wu, *et al.*, High efficiency and high color purity blue-emitting $NaSrBO_3$: Ce^{3+}phosphor for near UV light-emitting diodes, *J. Mater. Chem.*, 2011, **21**, 6869–6874.

21 X. Y. Huang, J. Liang, X. X. Li and A. He, Manipulating Upconversion Emission of Cubic Bagdf5:$Ce^{3+}/Er^{3+}/Yb^{3+}$ Nanocrystals through Controlling Ce^{3+} Doping, *J. Alloys Compd.*, 2017, **721**, 374–382.

22 D. Pasiński, E. Zych and J. Sokolnicki, Ce^{3+} to Mn^{2+} Energy Transfer in $Sr_3Y_2Ge_3O_{12}$: Ce^{3+}, Mn^{2+} Garnet Phosphor, *J. Alloys Compd.*, 2015, **653**, 636–642.

23 R. A. Talewar, S. Mahamuda, A. Vyas, A. S. Rao and S. V. Moharil, Enhancement of 1.54 mm Emission in Ce^{3+}/Er^{3+} Codoped $Ca_4si_2o_7f_2$ Phosphor, *J. Alloys Compd.*, 2019, **775**, 810–817.

24 D. W. Cooke, B. L. Bennett and R. E. Muenchausen, Intrinsic ultraviolet luminescence from Lu_2O_3, Lu_2SiO_5 and Lu_2SiO_5: Ce^{3+}, *J. Lumin.*, 2004, **106**(2), 125–132.

25 H. Suzuki, T. A. Tombrello, C. L. Melcher and J. S. Schweitzer, Light Emission Mechanism of $Lu_2(SiO_4)O$: Ce, *IEEE Trans. Nucl. Sci.*, 1993, **40**, 380–388.

26 D. Wen, J. Shi, M. Wu, *et al.*, Studies of terbium bridge: saturation phenomenon, significance of sensitizer and mechanisms of energy transfer, and luminescence quenching, *ACS Appl. Mater. Interfaces*, 2014, **6**(13), 10792–10801.

27 J. Chen, C. Guo, Z. Yang, *et al.*, Li_2SrSiO_4: Ce^{3+}, Pr^{3+} Phosphor with Blue, Red, and Near-Infrared Emissions Used for Plant Growth LED, *J. Am. Ceram. Soc.*, 2016, **99**, 218–225.

28 T. Katsumata, T. Nabae, K. Sasajima, *et al.*, Effects of Composition on the Long Phosphorescent $SrAl_2O_4$: Eu^{2+}, Dy^{3+} Phosphor Crystals, *J. Electrochem. Soc.*, 1997, **144**, L243–L245.

29 G. Che, C. Liu, X. Li, *et al.*, Luminescence properties of a new Mn^{2+} activated red long-afterglow phosphor, *J. Phys. Chem. Solids*, 2008, **69**, 2091–2095.

30 C. Liu, G. Che, Z. Xu, *et al.*, Luminescence properties of a Tb^{3+} activated long-afterglow phosphor, *J. Alloys Compd.*, 2009, **474**, 250–253.

31 E. W. Forsythe, D. C. Morton, C. W. Tang and Y. L. Gao, Trap states of tris-8-(hydroxyquinoline) aluminum and naphthyl-substituted benzidine derivative using thermally stimulated luminescence, *Appl. Phys. Lett.*, 1998, **73**, 1457–1459.

32 M. Shi, D. Zhang and C. Chang, Dy^{3+}: Ca_2SnO_4, a new yellow phosphor with afterglow behavior, *J. Alloys Compd.*, 2015, **639**, 168–172.

33 Z. Q. Liang, J. S. Zhang, J. S. Sun, X. P. Li, L. H. Cheng, H. Y. Zhong, S. B. Fu, Y. Tian and B. J. Chen, Enhancement of green long-lasting phosphorescence in $CaSnO_3$: Tb^{3+} by addition of alkali ions, *Physica B*, 2013, **412**, 36–40.

34 R. Chen, Glow curves with general order kinetics, *J. Electrochem. Soc.*, 1969, **116**, 1254–1260.

35 J. Y. Kuang and Y. L. Liu, Luminescence properties of a Pb^{2+} activated long-afterglow phosphor, *J. Electrochem. Soc.*, 2006, **153**, G245–G247.

